Comparison of Reaction Mechanisms of Epoxy Resins Undergoing Thermal and Microwave Cure from in Situ Measurements of Microwave Dielectric Properties and Infrared Spectroscopy

Eva Marand,* Kenneth R. Baker, and Jack D. Graybeal

Department of Chemistry, Virginia Polytechnic Institute and State University, Blacksburg, Virginia 24061-0212

Received July 3, 1991; Revised Manuscript Received December 19, 1991

ABSTRACT: New methods have been developed which enable one to monitor in situ the changes in the dielectric and spectroscopic properties of epoxy materials as they undergo cure by microwave as well as by thermal energy. In situ measurements at 2.45 GHz of the complex dielectric constant and of the infrared spectra of a DGEBA/DDS system undergoing isothermal cure at a number of temperatures have been conducted. Results have shown that although microwave radiation accelerates the curing reaction during early stages of the process, the induced rapid cross-linking creates a molecular network which is rigid enough to trap unreacted functional groups, thus actually causing a lower degree of cure. The cross-linking in samples cured by microwave radiation is caused by an accelerated reaction of the secondary amine group whose reactivity becomes similar to that of the primary amine.

I. Introduction

Epoxy resins are widely used in diverse applications such as surface coatings, printed circuit boards, the potting of electrical components, rigid frames, adhesives, and fiber-reinforced composites.[1] Advanced composites, in particular, have important use as replacements for metal in the production of commercial and military aerospace parts. The manufacture of such composites typically relies on conventional thermal curing of the matrix material. However, the application of thermal heating may pose processing problems such as long curing times and large temperature gradients, particularly in thicker samples.[2] Thus, alternative processing methods have been sought. Interest has evolved in the application of electromagnetic radiation in the microwave frequency range which generates heat directly within the sample. Possible advantages of microwave processing are higher efficiency, faster production rate, lower cost, more uniform cure, and improved physical/mechanical properties.[2,3] Several research efforts have been initiated in this area,[4-10] but none have truly addressed the difference in the chemistry and the curing mechanism on a molecular level for samples cured by microwave vs thermal energy. It is not known, for example, whether the preferential orientation of the dipoles in the microwave field, as opposed to the random orientation in the thermal field, could alter the rates of reactions in the curing process and thus lead to a different network morphology and properties. This question was posed in a recent paper by Mijovic and Wijaya.[10] Other investigators have introduced the notion of instantaneous local "hot" sites which may result within the material as the microwave energy modifies or surmounts the activation barrier of the potential chemical reaction at the site of the dipole.[9] However, these were only speculations without proof. Thus, until now, no direct experimental evidence on the actual molecular mechanism of cure has been offered.

We have developed techniques which enable us to monitor in situ the changes in the dielectric properties of epoxy materials as they undergo cure by microwave as well as by thermal energy. These techniques are based on a cavity perturbation method. A sample in the waveguide cavity can be cured via a microwave generator or a hot nitrogen gas source while its dielectric constant is periodically measured. We have also monitored in situ the molecular changes of the epoxy materials using Fourier transform infrared (FTIR) spectroscopy. As described below, we can monitor the cure of epoxy as it undergoes thermal cure or cure induced by microwave radiation.

Measurements of dielectric properties have been used to monitor chemical reactions for more than 60 years.[11] Traditionally, most of these studies are carried out in the more accessible radio frequency range below 100 MHz. In this frequency range most polymers and polymer composites exhibit relaxation dispersions at room temperature. Only a few investigations have focused on the microwave dielectric properties of polymeric materials.[12,13] However, recent advances in instrumentation have made such measurements more accurate and convenient.

There are advantages in using higher frequency dielectric measurements to study chemical reactions. At frequencies below 100 MHz, the interpretation of dielectric data in terms of the true physical properties of the reacting system is hampered by interfacial and electrode polarization. At microwave frequencies such effects are eliminated through the use of waveguides, and hence the dielectric data tend to reflect better the chemical and morphological state of the system. Additionally, the primary molecular response to the application of electric fields from the microwave frequency region is that of orientational polarization. Therefore, the dielectric properties are determined by the number of polar groups present in the sample and their relative mobility within the matrix material. As the curing proceeds in an epoxy formulation, one expects both the dielectric constant and the dielectric loss factor to decrease. This decrease would be a consequence of the reaction of and the subsequent decrease in the number of functional polar end groups as well as a decrease in molecular mobility resulting from the formation of a cross-linked network. In this study we observe and compare this decrease in complex dielectric constant for thermally cured samples with those for samples cured by microwave radiation.

In addition to dielectric measurements, we have also employed FTIR spectroscopy using infrared optical fibers. These fibers can be embedded in the epoxy matrix and permit us to monitor in situ the extent of reaction via observation of the changes in the characteristic infrared absorption bands.[14-16] Using this technique, we are able to compare the kinetics and the curing mechanism on a molecular level of samples cured by thermal heating and

0024-9297/92/2225-2243$03.00/0

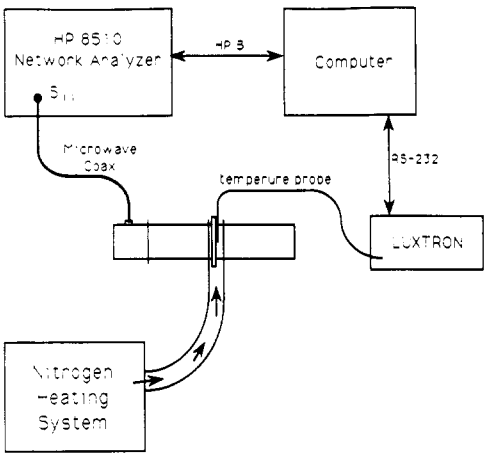

Figure 1. Experimental arrangement for dielectric measurements.

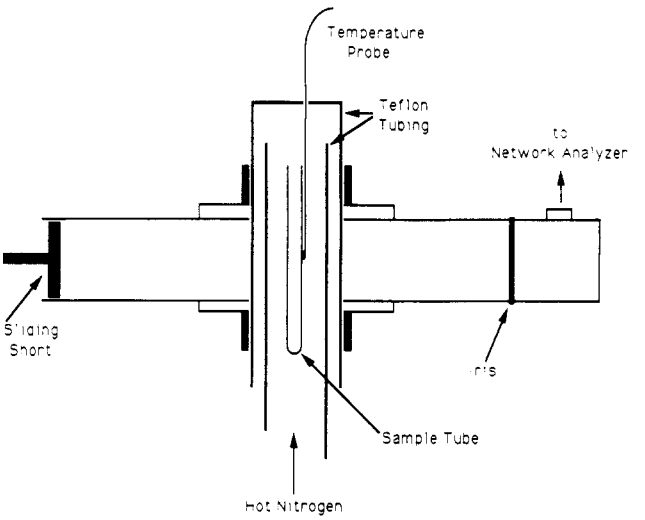

Figure 2. Cross-sectional view of the microwave cavity with magnified sample compartment.

by microwave fields. The combination of the dielectric measurements and FTIR observations has permitted a unique glimpse at the mechanism of cure under thermal heating and microwave heating conditions.

II. Experimental Section

A. Materials. An epoxy system consisting of diglycidyl ether of bisphenol A (DGEBA) and 4,4-diphenyldiamine sulfone (DDS) was investigated. The DGEBA (Dow Chemical) was recrystallized in 2-ethoxyethyl ether/methyl isobutyl ketone and dried for a week under vacuum at room temperature to remove water and remaining volatile solvents. The 4,4-DDS (Aldrich) was recrystallized in MeOH/H_2O and dried under vacuum for 2 days at room temperature. The 4,4-DDS was added to degassed DGEBA at 120 °C in stoichiometric ratio (1:2) and allowed to dissolve. The epoxy formulation was then transferred by a preheated pipet into a preheated NMR tube. High-precision NMR tubes were the standard sample holders in all of our dielectric measurements.

B. Methods. The work reported here is based on the results from four basic experiments: (1) measurements of the changing dielectric properties with time as the epoxy undergoes thermal cure; (2) measurements of the changing dielectric properties with time as the epoxy undergoes microwave cure; (3) observation of the changes in infrared absorption bands with time as the epoxy undergoes microwave cure; (4) observation of the changes in infrared absorption bands with time as the epoxy undergoes thermal cure. Each of these experiments was repeated at a set of constant temperatures that ranged from 140 to 200 °C. All dielectric measurements and microwave curing have been performed at 2.45 GHz. All experiments and data collection were entirely computer controlled and operated in the manner described below.

1. Dielectric Measurements with Thermal Cure. Figure 1 is a block diagram illustrating the arrangement of the experimental apparatus. A specialized waveguide cavity has been constructed to perform these measurements. Figure 2 shows a cross-sectional view of the rectangular cavity (largely magnifying the sample compartment) and the placement of the sample. We use a one-port rectangular cavity resonant in the TE_{103} mode. The cavity is made of brass WR-430 waveguide with a sliding short terminating one end and the input coupled to the network analyzer via an inductive iris. The waveguide was modified, top and bottom, with the addition of a shorted radial transmission line in combination with a 1 in. long circular waveguide to minimize the effects of the $^7/_{16}$ in. diameter hole. The hole permits sample insertion and the introduction of hot nitrogen for thermal heating. Our cavity heating arrangement is similar to that given in ref 17 except for the methods of temperature measurement and minimizing hole effects.

The temperature of the sample was monitored via a Luxtron Model 750 fluoroptic probe. The temperature of the N_2 gas was controlled by the gas flow rate and the settings on a Techne Fluidised Bath SBL-1 through which the gas was circulated. The nitrogen gas was passed around the sample twice, first by the inner wall and then by the outer wall of the Teflon tubing, to minimize any temperature gradients along the sample. Temperature gradients and temperature fluctuations with time were less than 3 °C inside the cavity.

The complex dielectric constant, $\epsilon = \epsilon' + j\epsilon''$, was measured using a cavity perturbation technique.[17,18] The geometry of the cavity in combination with the particular electromagnetic field mode that is excited (TE_{103} in this case) determines the resonant frequency and the Q of a particular cavity. The cavity Q is a measure of the energy losses that exist in the cavity. The cavity perturbation technique assumes that the introduction of the sample into a resonant cavity causes a small perturbation in the fields inside. Perturbations in the electromagnetic fields can be sensed by measurements of the resonant frequency and Q assuming the cavity dimensions are constant. Thus, to determine the dielectric constant, we have measured the changes in the resonant frequency and Q. The theory for deriving values of dielectric constant from changes in the resonant frequency and Q is well developed.[18,19] It should be pointed out that the power input into the cavity for the purpose of dielectric measurement is less than 10 mW. This is at least 3 orders of magnitude smaller than the power necessary to actually cure the sample.

Using an HP8510 vector network analyzer (NA) under computer control, the cavity was swept and the input reflection coefficient was measured. When the sweep was completed, the coefficients were transferred to the computer. There, they were processed to derive the resonant frequency and the Q. We then introduced the sample into the cavity and measured the resonant frequency and Q again. With this information the computer then calculated ϵ' and ϵ'' using the equations

$$\epsilon'_s = 1 + \frac{1(\omega_0 - \omega_s)V_{cav}}{2\omega_0 V_{sam}} \quad (1)$$

$$\epsilon''_s = \frac{1}{4}\left(\frac{1}{Q_0} - \frac{1}{Q_s}\right)\frac{V_{cav}}{V_{sam}} \quad (2)$$

where ϵ'_s and ϵ''_s are the real and imaginary parts of the relative dielectric constant of the sample, ω_0 and ω_s are the resonant frequency of the empty and perturbed cavity, respectivity, Q_0 and Q_s refer to the the empty and perturbed cavity, and V_{cav} and V_{sam} are the volumes of the cavity and of the sample, respectively.

As the epoxy was being prepared, the fluidized bath was brought to the desired temperature. An empty NMR tube, with fluoroptic temperature probe attached, was placed in the hot N_2 stream. The computer program was loaded, and the NA was calibrated. When all was ready, the system began by measuring the "empty" cavity approximately 30 times and calculated the average resonant frequency and average Q. These average values of the empty resonant frequency and the Q_0 were used throughout the remainder of the experiment. The systems then waited so

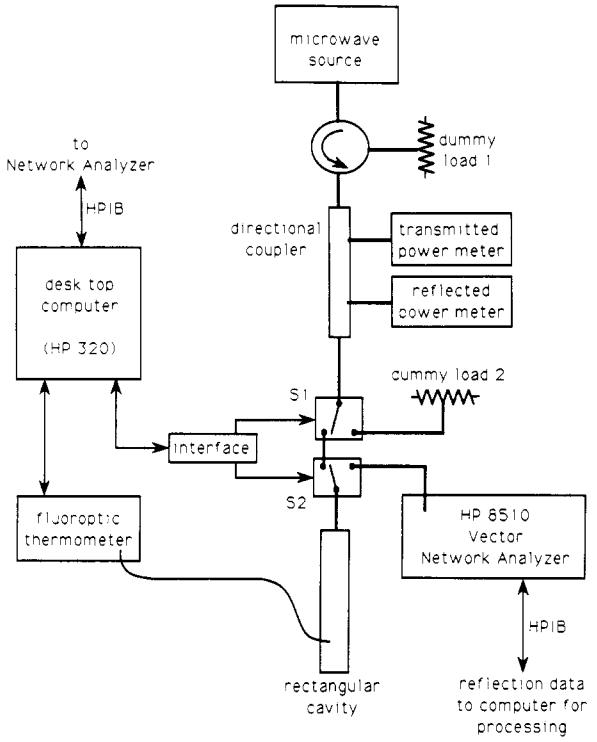

Figure 3. Experimental arrangement for combined microwave cure and measurement of the complex dielectric constant.

that the sample can be added to the empty NMR tube. On command, the experiment continued with the system first measuring the temperature and then immediately the dielectric constant. This process took approximately 7 s. At this point the system waited a predetermined time before taking the next measurement. This sequence continued for the duration of the experiment. The wait time between measurements was user selectable. In our experiments dielectric measurements were made once every minute for the first 20 min and then slowed to once every 3 min for the duration of our 3-h experiment.

2. Dielectric Measurements with Microwave Cure. Combined microwave cure and measurement of the complex dielectric constant was carried out using the experimental setup shown in Figure 3. The microwaves were generated by a Raytheon microwave power generator Model PGM-10X1 operating at a nominal frequency of 2.45 GHz. Using a coaxial cable, the source was connected to an isolator consisting of the circulator and dummy load 1. The isolator prevents any reflected power from damaging the source. The isolator was connected directly to a 20-dB directional coupler arrangement. The coupler, attenuators (not shown), and HP 435B power meters permit the transmitted and reflected power to be monitored. The output of the directional coupler was connected to switch 1 (S1) via coaxial cable. S1 and S2 are Narda SEM123D RF coaxial switches connected in the back to back arrangement shown. This arrangement was mounted directly at the input to the rectangular cavity with the switches S1 and S2 connected via a 1-in. section of semirigid coaxial cable. This circuit eliminated the possibility of applying high-power radiation to the front end of the NA whose maximum input is 100 mW.

This experiment measured the dielectric constant under thermal cure. The same cavity as described previously was used. The switches alternatively attached the NA to the cavity to make a dielectric constant measurement and then connected the high-powered microwave source to perform curing during the wait periods between dielectric constant measurements. The temperature of the sample was preset and held constant by the computer. S1 and S2 were used to selectively direct the microwave power to enter the cavity or direct the power to dummy load 2. Feedback from the fluoroptic thermometer to the computer initiated control of the switches. The variation in the sample temperature remained within ±1 °C. The fluoroptic thermometer supplied a temperature measurement to the computer every 0.4 s. Thus, the shortest pulse of microwave energy would have been 0.4 s given that the computer supplied microwave energy to the sample and then immediately decided to remove it after receiving the next temperature update. This was not typically the case. The power applied to the cavity was approximately 20 W or less in all of these experiments. Finally, although the empty NMR tubes which normally hold the sample also heated up in the microwave cavity, the rate of this heating was orders of magnitude lower than that observed for an NMR tube with the epoxy formulation inside.

3. FTIR with Microwave Cure. Infrared remote sensing experiments were conducted on a Nicolet 800 FTIR spectrometer on samples as they were subject to microwave radiation. The experimental setup was fundamentally the same as for the microwave experiment except that an FTIR instrument was interfaced instead of the HP network analyzer. The HP computer and the switches maintained a constant temperature. A 15-in. sapphire fiber (Galileo) was long enough to pass through the microwave cavity. This fiber was connected between two HMFG optical fibers by standard SMA fiber optic couplers. One end was positioned at the focal point of the incoming IR beam, and the other fiber focused the exit beam back into the MCT detector. The exposed sapphire fiber was immersed in the epoxy formulation contained in a Teflon sample holder fitted into the microwave cavity. Temperature was monitored via a fluoroptic probe immersed directly in the epoxy. Because the sapphire fiber has a T_m = 2000 °C, it was reused by burning off excess cured resin with a blow torch. In addition, the sapphire fiber has a low dielectric loss factor (approximately 1×10^{-4} [20]), and hence its presence within the cavity does not perturb the microwave heating of the sample.

However, there were disadvantages in using the exposed sapphire fiber. First, the signal to noise ratio was much lower than that in the transmission spectra, making precise quantitative analysis difficult. Second, after repeated use, the fiber began to degrade and a very sharp band was observed at 3280 cm^{-1} for the clean fiber, which interfered with our measurements of the NH_2 concentration. Finally, the fibers are very brittle and break easily. Due to breakage and the high cost of replacement, we were only able to carry out measurements for three different temperatures under microwave cure (140, 166, 195 °C) and for two temperatures under thermal cure (140, 166 °C). As the lower frequency limit of the optical fiber setup is 2400 cm^{-1}, we could only measure changes in the intensity of peaks such as 3386 cm^{-1} associated with the N–H stretch and 3560 cm^{-1} associated with a hydroxyl group which formed when the amine and epoxide react.

4. FTIR with Thermal Cure. Thermal curing kinetics were also studied by infrared spectroscopy, both in the transmission mode and through the use of remote sensing fibers. FTIR experiments in the transmission mode were conducted on a Nicolet 5 SXB FT-IR spectrometer using a Spectra Tech high-temperature cell. Changes in the characteristic epoxide absorption peak at 915 cm^{-1} were measured, corrected for thickness fluctuations using a reference band at 1507 cm^{-1}, and normalized. The results were correlated with the dielectric measurements of thermally cured epoxy samples.

For comparison, the optical fiber based remote sensing experiments were also performed as samples experience thermal curing. In this case, the optical fiber was passed through a glass rod wrapped with a heating tape to form a small thermal oven. A constant temperature was maintained through the use of a Nicolet temperature controller. The same type of Teflon sample holder was employed as used in the fiber optic microwave cure.

III. Results

The reaction mechanism and kinetics of the curing process determine to a great extent the final structure of the molecular network. In general, the epoxy curing process involves several reactions which can be very complex and the precise kinetics cannot be predicted with confidence for given compositions and conditions. Orders of reaction between 0 and 4 have been reported, and the apparent order may change during the reaction.[1,21,22] Furthermore, while early stages may show autocatalytic

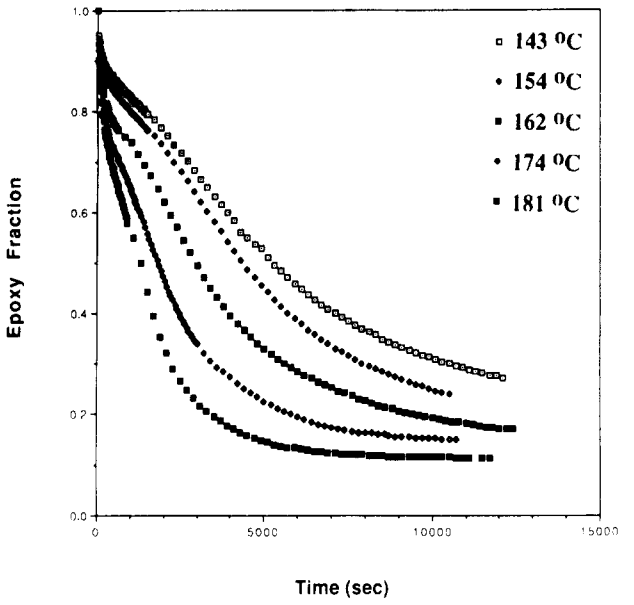

Figure 4. Results of transmission FTIR experiments during thermal cure based on changes in the 915-cm^{-1} band.

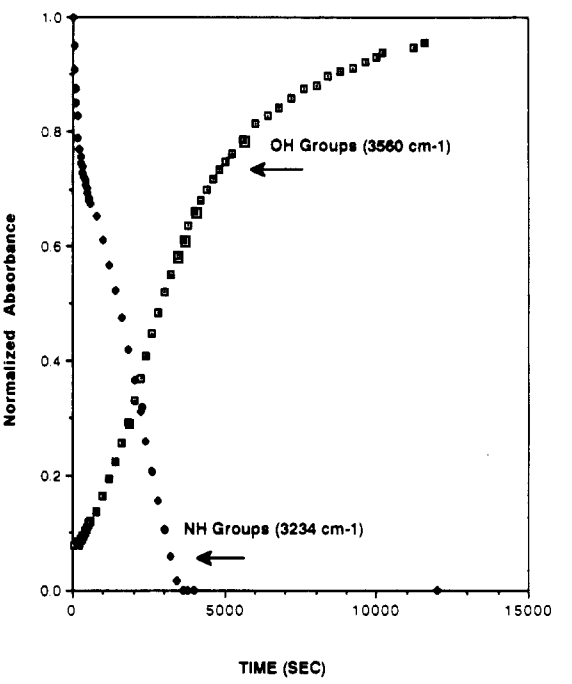

Figure 5. Results of transmission FTIR experiments during thermal cure based on changes in the 3560- and 3234-cm^{-1} bands.

features, the onset of gelation can introduce a degree of diffusion control to the kinetics.[22] Nevertheless, there are three basic reactions known to occur which we can use, at least qualitatively, to explain the differences in the reaction mechanism between thermally cured and microwave cured epoxy formulations:

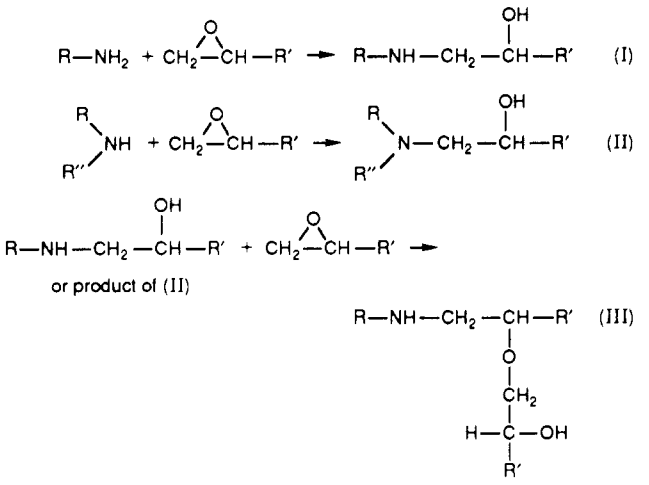

The epoxy moieties of the DGEBA can react with either the primary or the secondary amine to form an OH adduct, which can later react with another epoxide ring in an etherification reaction to further cross-link the resin. The tendency of the etherification reaction to take place depends on the temperature and increases with the initial ratio of epoxide/amine.[22,23] It has also been reported that etherification appears only after all of the amine has been consumed.[23] The relative rates of these individual reactions are especially important. In all of our discussions we have also assumed that the homopolymerization of the epoxy is negligible.[20]

Thermal Curing Process. The results of the transmission FTIR experiments of thermal cure are shown in Figure 4. Examination of the epoxide fraction profile for various temperatures shows that there are three regions present. The first region shows a relatively slow decrease of the epoxy moiety and an exhaustion of the NH_2 groups. An example of the change in the NH_2 concentration as measured by the area of peak 3234 cm^{-1} is shown in Figure 5. We postulate that this region corresponds to the reaction of a primary amine with an epoxy group of the DGEBA. The second region is marked by a rapid decrease in the epoxide concentration and a steady rise of the hydroxyl moiety also as shown in Figure 5. We expect this behavior to be associated with the second reaction, namely of the secondary amine with the epoxy group. The system also begins to cross-link via this reaction, slowing down the ability of the end groups to find each other and react. Hence, toward the end of this region, the decrease in epoxy groups and the rise in hydroxyl groups begin to slow down. The third region occurs when the sample vitrifies and the reaction of the epoxide groups becomes diffusion limited. Since the etherification reaction is supposedly catalyzed by the tertiary amine,[23] we would expect this reaction to occur, if at all, toward the end of the second region and throughout the third region. As expected, although the rates of all of the individual reactions increase with temperature, one can still identify the three regions.

The dielectric storage factor (ϵ') and the dielectric loss factor (ϵ'') as a function of curing temperature and time are shown in Figure 6. These two properties reflect the ability of the molecular dipole moments in the material to follow the oscillations of an applied electric field. While the dielectric constant represents the component of immediate alignment of the dipole moments in the direction of the electric field, the dielectric loss factor reflects the retardation incurred in the rearrangement. Hence, the changes in the dielectric properties should reflect not only the alterations in molecular dipole moments as a result of chemical reactions taking place but also the rapid decrease in molecular mobility that occurs during the formation of a cross-linked network. Initially, the dielectric properties of the epoxy system increase as the sample temperature reaches that of the

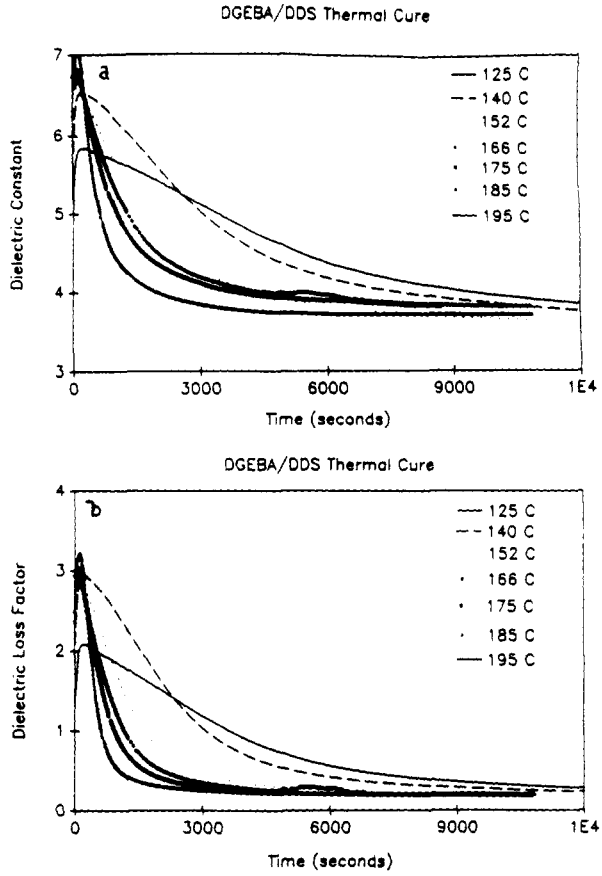

Figure 6. Dielectric storage factor (a, E') and dielectric loss factor (b, E'') during thermal cure as a function of time.

preheated sample holder and then decrease with the onset of curing. The magnitudes of the dielectric properties, particularly at the beginning of the curing process, are larger at higher curing temperatures. This effect is diminished as the reaction proceeds, although the influence of temperature is still observed even in fully cured samples. This observation is illustrated in Figure 7 for a sample cured at T = 180 °C for 3 h.

Comparison of the dielectric properties of the epoxy undergoing cure with the dielectric properties of the pure components at corresponding temperatures suggests that the diamine contributes substantially to the magnitude of ϵ' and ϵ'' of the epoxy system. This is in agreement with previous kinetic studies which have calculated the dipole moments of the reacting polar groups as 7.6×10^{-30} C·m for the epoxide, 14.8×10^{-30} C·m for the primary amine, and 12.6×10^{-30} C·m for the reacted amine.[11] The dipole moment of the hydroxyl group may be slightly higher than that of the epoxy ring.[24]

Parts a and b of Figure 8 show the relationship between the epoxy fraction and the dielectric storage factor and the dielectric loss factor, respectively. These relationships were obtained by cross-correlating the FTIR transmission data and the dielectric data using time as a common denominator. Both curves are characterized by an initial rapid decrease of the dielectric properties with a slow change in dielectric properties above 50% extent of reaction (extent of reaction = 1 − epoxy fraction). We explain this behavior on the basis of theoretical considerations. Unfortunately, the quantitative theories that relate the relaxed dielectric constant to the concentrations and dipole moments of the various polar end groups are insufficient to deal with polymers, where intermolecular and intramolecular forces, as well as entanglements, play

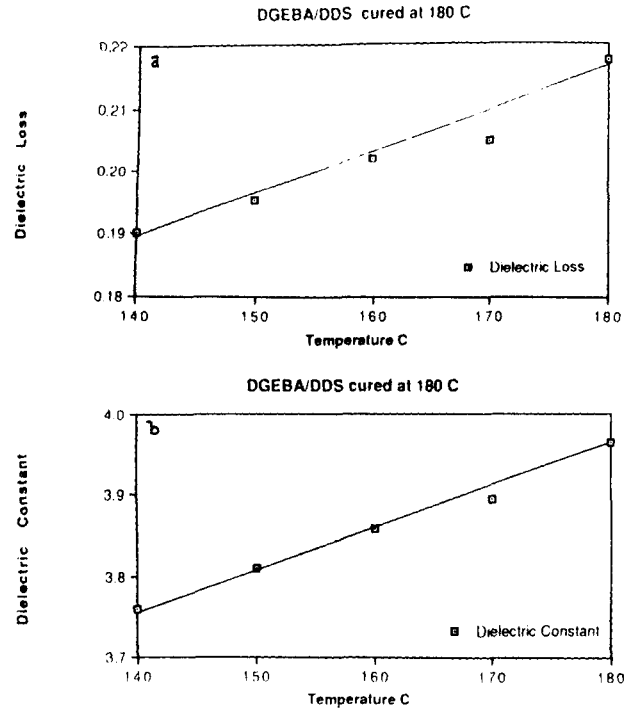

Figure 7. Dielectric loss factor (a) and dielectric storage factor (b) as a function of temperature for fully cured sample.

a role.[25,26] However, we deem it reasonable to assume that the dielectric properties will scale with $\sum N_i(\mu_i)^2$, where N_i is the number of polar groups of particular species i and μ_i is the corresponding dipole moment. On the basis of our previous consideration of the reaction chemistry, the quantity $\sum N_i(\mu_i)^2$ must vary with the extent of reaction, α, as

$$\sum N_i(\mu_i)^2 = A'(1-\alpha) + B'\alpha + C' \tag{3}$$

where the constant A' represents primarily the dipole moment contribution of the epoxy groups and primary amine groups, as well as some contribution from secondary amine groups and hydroxyl groups. The constant B' represents primarily the contributions of the hydroxyl groups and the secondary and tertiary amine groups, and C' encompasses all dipole moment contributions not involved in the reaction process. On the basis of our previous discussion concerning the relative magnitude of the various dipole moments, we can safely assume that $A' > B'$. In this case, eq 3 can be reduced to

$$\sum N_i(\mu_i)^2 = N = N_0 - k\alpha \tag{4}$$

where N_0 and k are constants having units of (C·m)^2. Hence, the dielectric properties should decrease linearly with the extent of reaction if ϵ' and ϵ'' depend primarily on the concentration of the polar end groups. The fact that this is not the case suggests that the dielectric properties must also reflect the changes in the relaxation time, τ, which will increase with the extent of reaction as the cross-linking restricts the polymer matrix. The relationship between the dielectric properties and the relaxation time is given by the Debye equation[25,26]

$$\epsilon'(\omega) = \epsilon_\infty + (\epsilon_s - \epsilon_\infty)/(1 + \omega^2\tau^2) \tag{5}$$

$$\epsilon''(\omega) = [(\epsilon_s - \epsilon_\infty)/(1 + \omega^2\tau^2)]\omega\tau \tag{6}$$

where ϵ_s is the static dielectric constant and ϵ_∞ is the instantaneous dielectric constant.

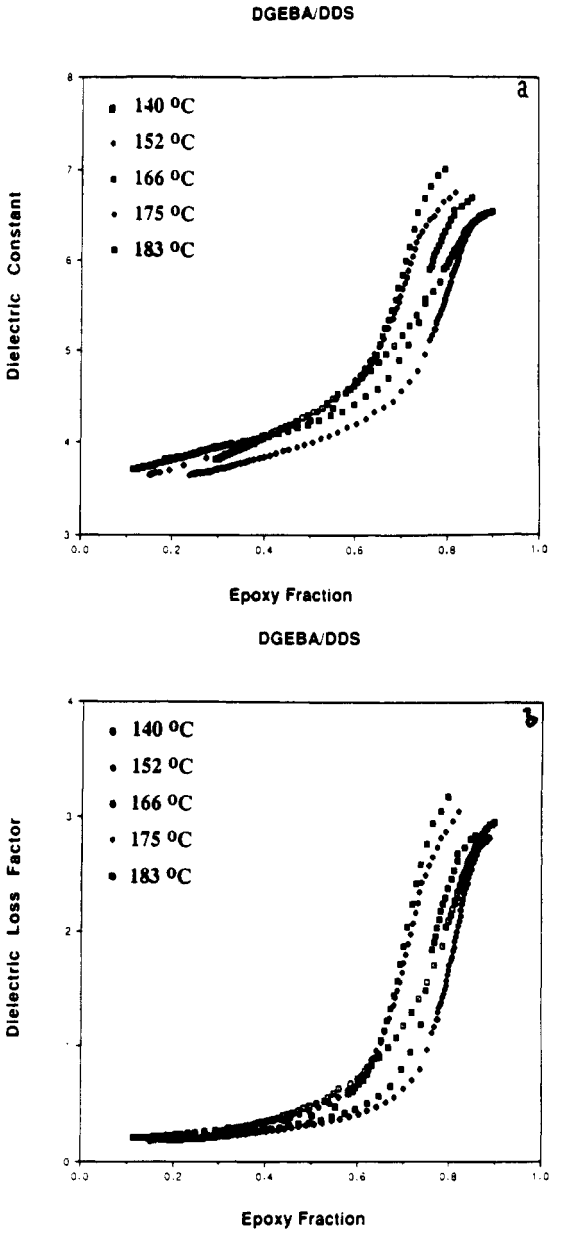

Figure 8. Dielectric storage factor (a) and dielectric loss factor (b) as a function of the epoxy fraction during thermal cure.

Since in a curing reaction the relaxation time will vary from about 1×10^{-8} s to 1 h over the course of an isothermal curing experiment,[27] the contribution of the $1/(1 + \omega^2\tau^2)$ term will diminish with time. Therefore, at long times, ϵ' will approach ϵ_∞ and ϵ'' will approach zero. This is what we observe experimentally.

Because $\omega = 15.4 \times 10^9$ s^{-1}, we assume that $\omega^2\tau^2 > 1$ and let

$$\epsilon' = N[a_0 + (a_1/\tau^2)] \tag{7}$$

$$\epsilon'' = a_2(N/t) \tag{8}$$

where a_0, a_1, and a_2 are constants.

Because the relaxation time will change with the extent of reaction, α, a model for the curing reaction of epoxy resins developed by Matsuoka et al.[27] has been used in our analysis:

$$\tau = D \exp[C(T)/1 - (A + B\alpha)] \tag{9}$$

This model is derived from the Adam and Gibbs[28] formula for relaxation phenomena in the equilibrium state. The relationship considers cooperative motions of molecular segments in domains of varying sizes, where the total configurational entropy, S, is the factor that determines the critical size for such domains:

$$\ln \tau = C + (\Delta\mu s^*/kTS) \tag{10}$$

Here, $\Delta\mu$ is the potential energy hindering the cooperative rearrangement of a smallest possible molecular unit having itself a configurational entropy, s^*. The total configurational entropy, S, is assumed to be equivalent to the quantity $s^*(1 - T_2/T_f)$, where T_2 is the temperature below which the equilibrium state cannot be reached. T_f is a fictitious temperature defined as the temperature at which the liquid state has been frozen to form a given glassy state.[27]

The constants T_{20} and $T_{2\infty}$ are defined as the values of T_2 at $t = 0$ and $t = \infty$, respectively. T_2 varies with the degree of cure as

$$T_2 = T_{20} + \alpha(T_{2\infty} - T_{20}) \tag{11}$$

Hence, the constants in eq 9 can be expressed as

$$A = T_2/T_f \qquad B = (T_{2\infty} - T_{20})/T \qquad C(T) = \Delta\mu/kT$$

Substituting eqs 4 and 9 in eqs 7 and 8, we obtain

$$\epsilon' = (N_0 - k\alpha)\left[a_0 + \frac{a_1}{\left[\exp\left[\frac{C(T)}{1 - (A + B\alpha)}\right]\right]^2}\right] \tag{12}$$

$$\epsilon'' = (N_0 - k\alpha)\left[\frac{a_2}{\exp\left[\frac{C(T)}{1 - (A + B\alpha)}\right]}\right] \tag{13}$$

We have used eqs 12 and 13 depicting the relationship between the dielectric properties and the extent of reaction to fit our data shown in Figure 8. For polymers, the hindrance energies of internal rotations, $\Delta\mu$, are expected to be a few kilocalories per mole.[28] Hence, we assume $C(T) = 1$ for our purposes. We also know that the sum of $A + B$ must be less than 1, because $T_{2\infty}/T_f < 1$.[27] Finally, $a_0(1 - k)$ is the value of the dielectric storage factor at long curing times when N_0 is normalized to 1 (since each sample begins with the same stoichiometry). Using a least-squares fitting routine[29] with a five-parameter fit, we calculate the constants of eq 12. These are shown in Table I.

Table I

	T, °C				
	140	150	160	170	180
k	0	0.067	0	0.03	0.137
a_0	2.24	3.86	3.48	3.72	4.24
a_1	1.65×10^5	1.98×10^5	1.75×10^5	2.18×10^5	2.36×10^5
A	0.805	0.81	0.805	0.806	0.798
B	0.054	0.088	0.097	0.074	0.110

Similarly, using a four-parameter fitting routine, we can fit the dielectric loss factor data. The original data along with the fitted curve are shown for one temperature, T = 160 °C, in Figure 9. These calculations show that the average value of the k constant is quite low. Because the k value reflects the relative contribution of the changes in the polar end group concentratitons to the dielectric properties, one can conclude that the nature of the decrease of the dielectric properties at microwave frequencies is predominantly dictated by the changes in the polymer superstructure and not as much by the changes in the polar end group concentration. In other words, the dielectric properties decrease as a result of the cross-linking

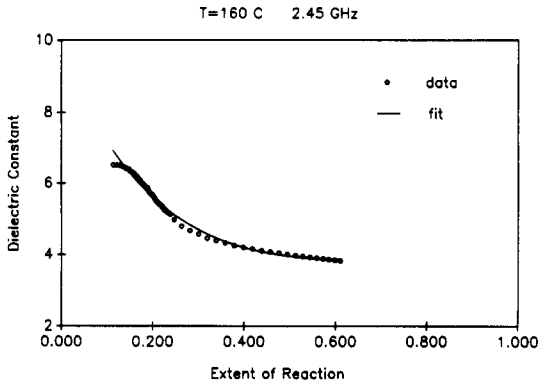

Figure 9. Theoretical fit of the dielectric constant for thermally cured samples.

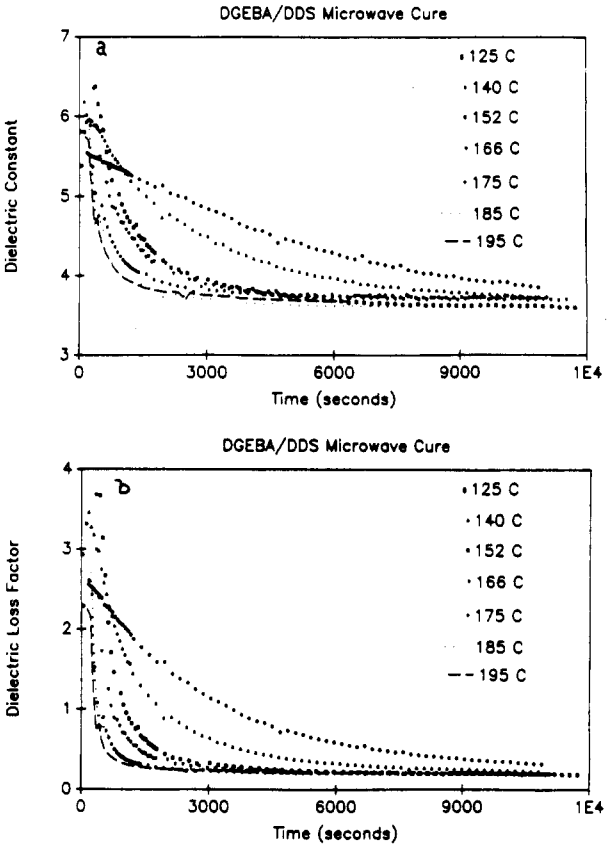

Figure 10. Dielectric storage factor (a) and dielectric loss factor (b) as a function of time for samples cured by microwave radiation.

and vitrification of the DGEBA/DDS epoxy system, a process which seems to restrict the response of the polar end groups to the microwave field.

Microwave Curing Process. Figure 10 shows the dielectric properties of the DGEBA/DDS epoxy system as it undergoes curing by microwave radiation at a number of different temperatures. As with the thermally cured samples, both the dielectric storage factor and the dielectric loss factor decrease exponentially with time. However, a close comparison of the dielectric data for both types of curing processes indicates a much more rapid decrease of the dielectric properties in the case of microwave-induced curing. Figures 11 and 12 compare individually the dielectric storage factors and the dielectric loss factors for both curing processes at the same temperature. These data show that the differences in the rate of decrease of the dielectric properties are greater at lower temperatures. On the basis of our previous discussion of the thermal data, we have concluded that the cross-linking begins

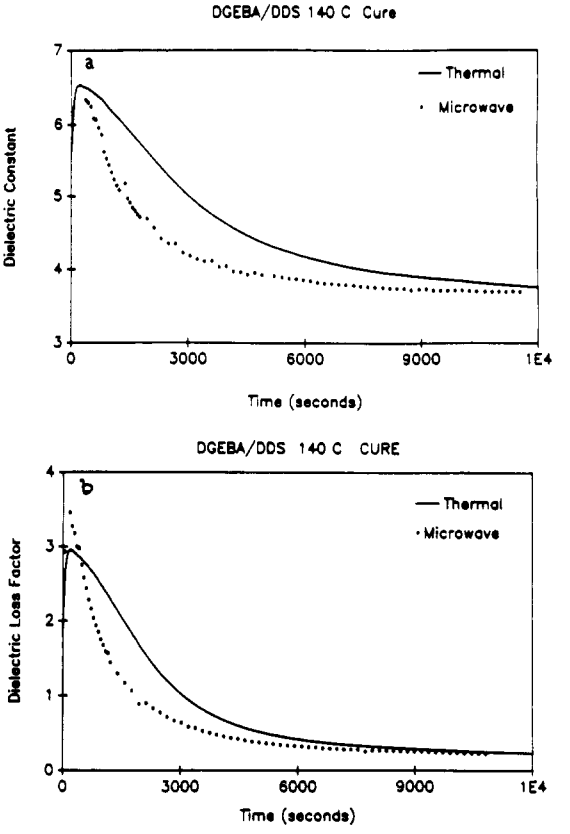

Figure 11. Comparison of the dielectric storage factor (a) and the dielectric loss factor (b) for thermally cured and microwave cured samples as a function of time.

sooner and is more rapid in those samples cured by microwave radiation than in those cured thermally. However, at higher temperatures, since all reactions proceed very quickly, any differences in the cross-linking rates become too subtle to detect via measurements of dielectric properties.

An example of an FTIR spectrum obtained during microwave curing studies using a sapphire fiber is shown in Figure 13a. For comparison we have included a spectrum obtained during thermal curing using the transmission method. This is shown in Figure 13b. The evolution of hydroxyl groups was followed by measuring the absorbance at 3561 cm^{-1} associated with the O–H stretch. These values were normalized to the peak height of the 3386-cm^{-1} band measured at the beginning of the experiment to correct for thickness (or area) variations. The relative appearance of the hydroxyl groups as a function of time during microwave curing is shown in Figure 14 for three different temperatures. Figures 15–17 compare the evolution of OH groups for thermally cured and microwave cured samples at similar temperatures.

At 140 °C, although the evolution of OH groups is greater during thermal curing, the differences between thermal cure and microwave cure are not as pronounced as those observed at higher temperatures. This suggests that at this lower temperature the reactions observed are principally those of the primary and secondary amine groups. The fact that at 140 °C the dielectric data show a more rapid rate of cross-linking during microwave curing points to a stronger involvement of the secondary amine reaction in the microwave curing process than in the thermal curing process. At temperatures above 150 °C the differences in the curing mechanisms of the two methods become much more pronounced. The evolution of the hydroxyl groups

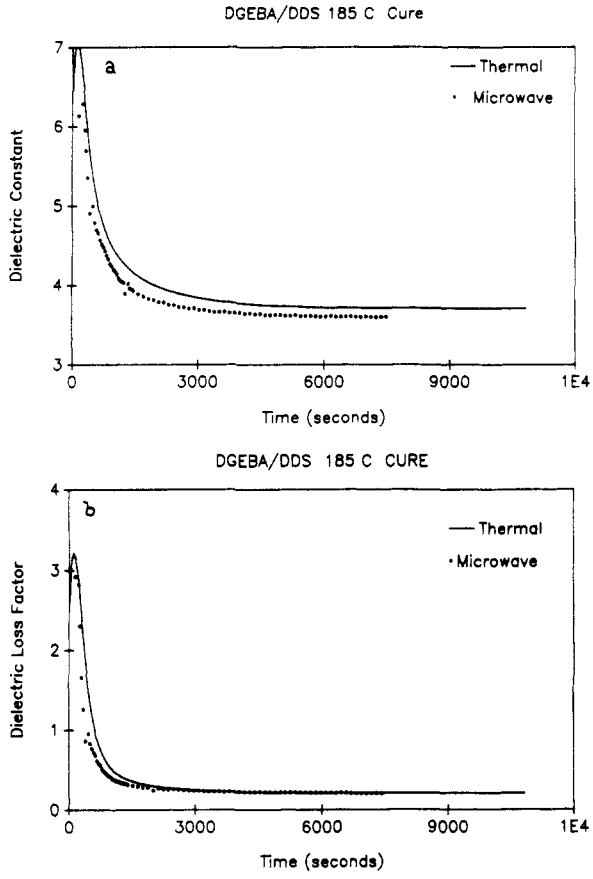

Figure 12. Comparison of the dielectric storage factor (a) and the dielectric loss factor (b) for thermally cured and microwave cured samples as a function of time.

during microwave heating appears to be more rapid during the early stages of the curing cycle and then quickly levels off to a constant value. On the other hand, the hydroxyl groups increase steadily throughout the thermal curing process. These results point to two possible mechanisms during the middle stages of microwave curing. The first possibility is that there is a participation of the etherification reaction which would maintain the concentration of OH groups constant. The other possibility is that there are no more reactions taking place because the system is already densely cross-linked. To find out which hypothesis is true, we have individually cured a number of epoxy formulations by microwave radiation for different periods of time and obtained their infrared transmission spectra by FTIR. The epoxy formulations were cast on FEP films, cured in the microwave cavity at 166 °C for 1, 2, and 2.5 h, and subsequently quenched in dry ice. In all cases the infrared spectra showed a large amount of unreacted epoxy moiety upon comparisons of the 915-cm^{-1} band with thermally cured samples at corresponding times. These results suggest that the etherification reaction indeed *does not* take place during microwave curing. In addition, we have observed unreacted amine groups in the transmission spectra as well as in the spectra obtained with the sapphire fiber of samples cured by microwave radiation, while none have been observed in the spectra of thermally cured samples. Unfortunately, the spectra obtained using the sapphire fiber were much too noisy in this frequency region to be used for accurate quantitative analysis. An example of these data is shown in Figure 18.

IV. Discussion

On the basis of these results we conclude that although microwave radiation accelerates the curing reaction during

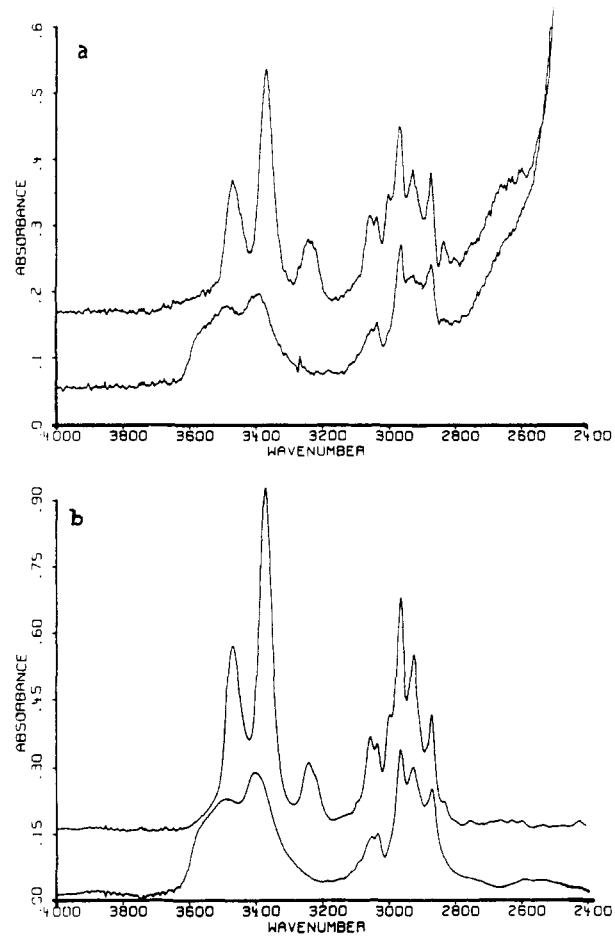

Figure 13. FTIR spectrum obtained during microwave curing studies using a sapphire fiber (a) and during thermal curing using transmission mode.

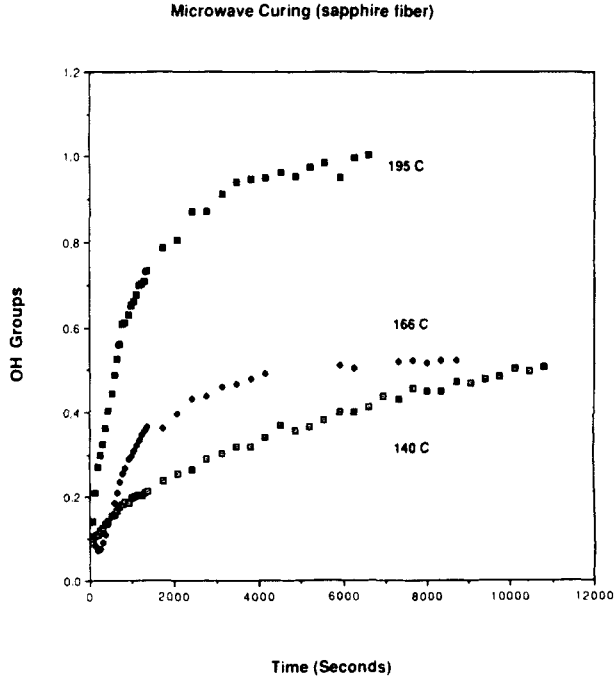

Figure 14. Changes in the hydroxyl group concentration during microwave curing.

early stages of the process, the rapid cross-linking creates a molecular network which is rigid enough to trap unreacted functional groups, thus actually causing lower degree of cure. The cross-linking must be caused by an accelerated

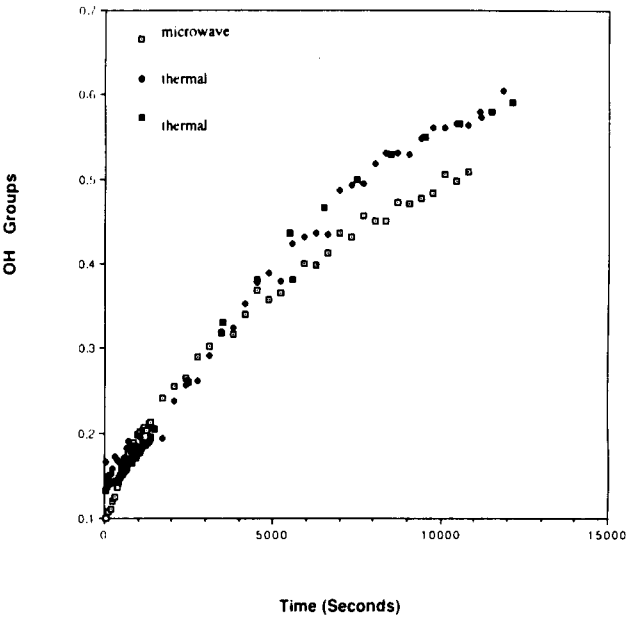

Figure 15. Comparison of the changes in the hydroxyl concentration for thermally cured and microwave cured samples.

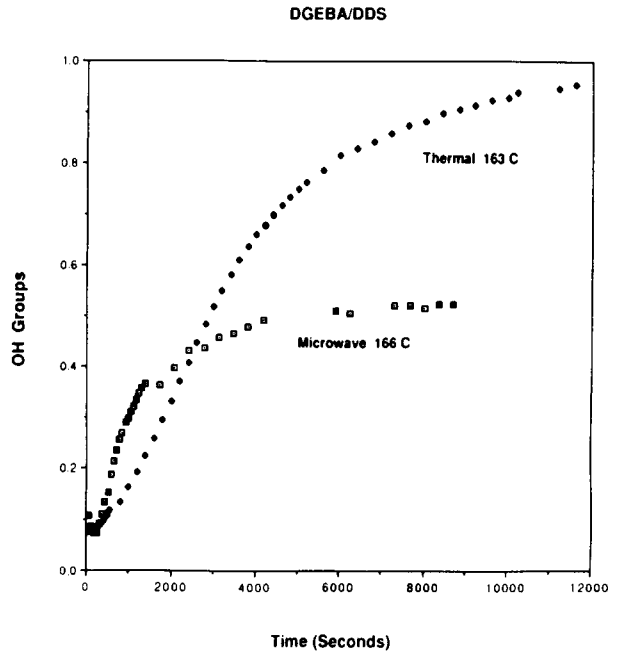

Figure 16. Comparison of the changes in the hydroxyl concentration for thermally cured and microwave cured samples.

reaction of the secondary amine group which is competing more effectively for the epoxy end groups than one would observe in thermally cure samples. Our results seem to be consistent with those of Mijovic et al.,[10] who have conducted a comparative calorimetric study of cure of an epoxy/amine (DGEBA/DDS) formulation by microwave and thermal energy. Their results have shown that the degree of cure and glass transition temperature increase faster in a thermal than a microwave field and that the microwave cured samples have a broader T_g range. However, they could not provide information about the molecular mechanism because DSC measurements cannot follow the heats of individual partial reactions. Other investigators have claimed a 20-fold increase in the rate of cross-linking of modified poly(ether ketone) (PEK) oligomers by microwaves as compared to thermal curing at the same temperature.[9] However, these results are in doubt because large field variation over the entire length of the sample has been observed in the particular cavity used.[30] Therefore, the temperature recorded may not have corresponded to the actual degree of gelation measured. In fact, the average glass transition temperatures reported in the same paper were much lower for those samples cured by microwave radiation than for those cured thermally.

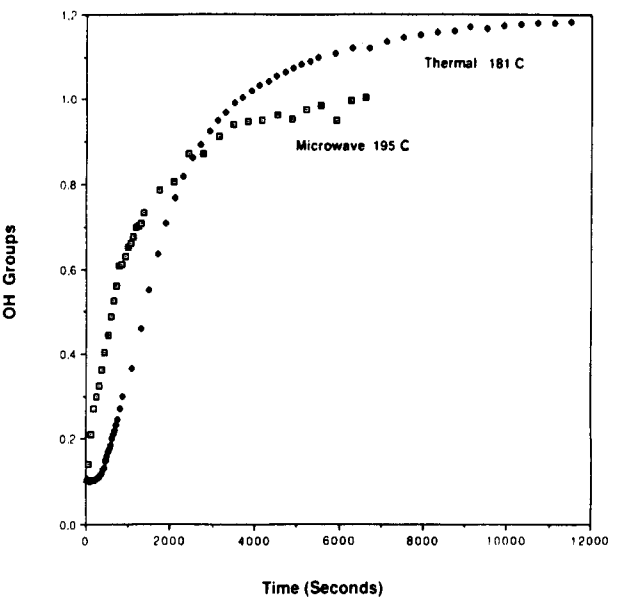

Figure 17. Comparison of the changes in the hydroxyl concentration for thermally cured and microwave cured smaples.

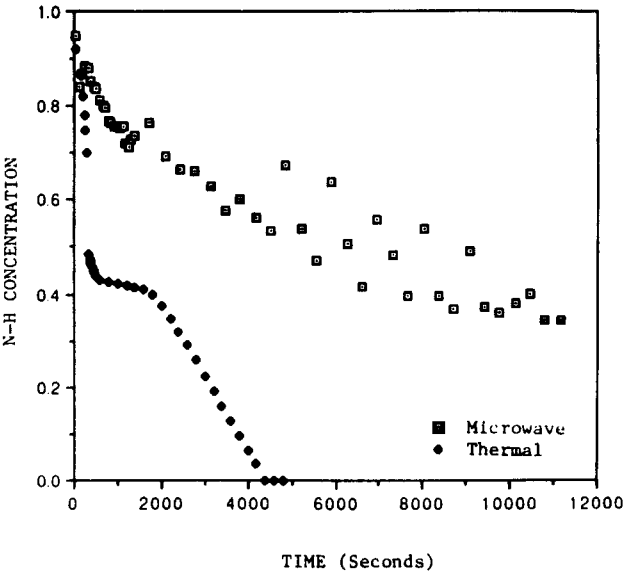

Figure 18. Changes in the N–H concentration for thermally cured and microwave cured samples.

We now have a better understanding of the differences in the reaction mechanism when comparing both cure methods, and we can theorize as to what the fundamental reasons for these differences are. One hypothesis is that the reactive groups, being highly polar in nature, are selectively activated toward reaction by microwave radiation. Under conventional conditions where heat is supplied from the outside, the entire molecule has to be excited before the end group can react. In general, the

secondary amino group is less reactive than the primary one, due to steric hindrances.[23] Under microwave excitation, however, there is a possibility that their reactivities become more similar. For example, small molecules in the gas phase and at low pressures have discrete absorption spectra due to rotation and in some cases the inversion of the molecules.[31] The inversion is particularly significant in ammonia and the amines. As the pressure is increased and a condensed phase is formed, the frequency range over which the absorption is observed becomes very broad.[32] It is expected that the inversion phenomenon would still be operative in the condensed phase because it involves the motion of the central nitrogen atom in the plane of the peripheral atoms, rather than the motion of the peripheral atoms. For this reason, amine-type molecules which have inversion frequencies lying in the range 4–26 GHz[33] will absorb appreciably at 2.45 GHz in the condensed phase. On the basis of this reasoning, one would expect the inversion motion to be similar in the primary and the secondary amines of the epoxy formulation. Hence, when placed in a microwave field, both types of amines would experience a comparable level of excitation. If the level of energy activation is high enough to overcome any steric effects, the reactivities of the two amino groups should be similar.

V. Conclusions

We have shown that for the epoxy system of DGEBA/DDS in stoichiometric proportions the rate of cross-linking is much higher in those samples cured by microwave radiation than in those cured thermally. Particularly at higher temperatures, this phenomenon appears to lead to entrapment of unreacted amine and epoxy groups within the resin matrix, leading to overall lower degree of cure in the microwave cured samples. It has to be pointed out, however, that these conclusions are particular to the epoxy system examined and that in other molecular systems, void of the possibility of cross-linking reactions, the acceleration of reactions by microwave radiation may effectively lead to higher degrees of reaction completion or overall faster reaction rates.

Acknowledgment. This work was supported by Air Force/DARPA Research Contract F33615-85-C-5153. We acknowledge Prof. James M. Tanko for helpful discussions concerning the epoxy cure mechanism. We are indebted to Prof. Tom Ward, Dr. John Hellgeth, and the NSF Science and Technology Center at Virginia Technical Institute for access to their FT-IR facilities and high-powered microwave source and equipment.

References and Notes

(1) Epoxy Resins and Composites *Adv. Polym. Sci.* **1985**, *72*, 75.
(2) Mijovic, J.; Wijaya, J. *J. Polym. Compos.* **1990**, *11* (3), 184.
(3) Jaw, J.; Di Long, J. E.; Hawley, M. C. *SAMPE Q.* **1989**, *20*, 46.
(4) Lee, W. I.; Springer, G. S. *J. Compos. Mater.* **1984**, *18*, 357, 387.
(5) Jullien, H.; Valot, H. *Polymer* **1985**, *26*, 506.
(6) Teffal, M.; Gourdenne, A. *Eur. Polym. J.* **1983**, *19*, 543.
(7) Le Van, Q.; Gourdenne, A. *Eur. Polym. J.* **1987**, *23* (10), 777.
(8) Jow, J.; Finzel, M.; Asmussen, J.; Hawley, M. C. *IEEE MTT-S Dig.* **1987**, *1*, 465.
(9) Hedrick, J. C.; Lewis, D. A.; Ward, T. C.; McGrath, J. E. *Polym. Prepr.* **1988**, *29* (1), 363, and references cited therein.
(10) Mijovic, J.; Wijaya, J. *Macromolecules* **1990**, *23* (15), 3671–3674.
(11) Sheppard, Norman F., Jr. *Adv. Polym. Sci.* **1986**, 80, 1–47, and references cited therein.
(12) Bur, A. J. *Polymer* **1985**, *26*, 963–977.
(13) Frosini, V.; Butta, E. *J. Appl. Polym.* **1967**, *11*, 527–551.
(14) Compton, D. A. C.; et al. *Appl. Spectrosc.* **1988**, *42* (6), 972.
(15) Young, P. R.; Druy, M. A.; Stevenson, W. A.; Compton, D. A. C. *SAMPE J.* **1989**, *25*, 11.
(16) Druy, M. A.; Elandjian, L.; Stevenson, W. A. *SPIE Proc.* **1988**, *986*, 130.
(17) Rzepecka, M. A. *J. Microwave Power* **1973**, *8* (1), 3.
(18) Altschuler, H. Dielectric Constant. *Handbook of Microwave Measurements*; Suchor, M., Fox, J., Eds.; Polytechnic Press: Brooklyn, NY, 1963; Vol. 2.
(19) Harrington, R. F. *Time-Harmonic Electromagnetic Fields*; McGraw-Hill: New York, 1961, Chapter 7.
(20) Gardiol, Fred E. *Introduction to Microwaves*; Artech House: Dedham, MA, 1984.
(21) Potter, W. G. *Epoxide Resins*; Springer-Verlag: New York, 1970.
(22) Pascault, J. P.; et al. *Macromolecules* **1990**, *23*, 725.
(23) Matyka, L.; Dusek, K. *Macromolecules* **1989**, *22*, 2902, and references cited therein.
(24) McClellan, A. L. *Tables of Experimental Dipole Moments*; Rahara Enterprises: El Cerrito, CA, 1989; Vol. 3.
(25) Blythe, A. K. *Electrical Properties of Polymers*; Cambridge University Press: Cambridge, 1979.
(26) McCrum, N. G.; Read, B. E.; Williams, G. *Anelastic and Dielectric Effects in Polymeric Solids*; Wiley: London, 1967.
(27) Matsuoka, S.; Quan, X.; Bair, H. E.; Boyle, D. J. *Macromolecules* **1989**, *22*, 4093–4098.
(28) Adam, G.; Gibbs, J. H. *J. Chem. Phys.* **1965**, *43* (1), 139–146.
(29) Fitting routine adapted from Bevington's *Data Reduction and Error Analysis*.
(30) Jabari, I. Master's Thesis, VPI&SU, August 1989.
(31) Gordy, W.; Cook, R. L. *Microwave Molecular Spectra*; Wiley: New York, 1984; Chapter 6.
(32) Townos, C. H.; Schowlow, A. L. *Microwave Spectroscopy*; McGraw-Hill: New York, 1965; Chapter 13.
(33) Nishikawa, T. *J. Phys. Soc. Jpn.* **1957**, 12 (6), 668–680.

Registry No. DGEBA (homopolymer), 25085-99-8; DDS, 80-08-0.